J Mater Sci (2014) 49:2875–2878
DOI 10.1007/s10853-013-7993-2

Effect of calcium on the structural properties of $Ba_{(1-x)}Ca_xTiO_3$ particles synthesized by complex polymerization method

V. D. Araújo · F. V. Motta · A. P. A. Marques · C. A. Paskocimas · M. R. D. Bomio · E. Longo · J. A. Varela

Received: 11 September 2013 / Accepted: 21 December 2013 / Published online: 14 January 2014

Abstract Ferroelectric materials, such as barium titanate ($BaTiO_3$), have been extensively studied for application in electronic and optical devices. The substitution of Ba by Ca is an effective method to improve the piezoelectricity temperature stability, as it can greatly lower the tetragonal–orthorhombic phase transition temperature, whereas the change of the Curie point is negligible. $Ba_{(1-x)}Ca_xTiO_3$ ($x = 0$, 0.05, 0.10, 0.15, and 0.20) powders were prepared by complex polymerization method. The effect of calcium on the tetragonality of the $BaTiO_3$ system was monitored using basic characterization techniques: X-ray diffraction, differential scanning calorimetry, and Raman spectroscopy. The results indicate that increased calcium contents raise the Curie temperature (T_c) and that the addition of calcium in the BT matrix reduces tetragonality.

Introduction

Ferroelectric materials have been extensively studied for application in electronic and optical devices. Among these materials, the barium titanate ($BaTiO_3$) perovskite presents excellent dielectric properties [1]. The substitution of Ba by Ca in the $BaTiO_3$ perovskite results in an improvement in the stability of piezoelectric properties, consequently the barium calcium titanate ($Ba_{(1-x)}Ca_xTiO_3$) solid solution has attracted great attention for its use in laser systems, piezoelectric devices, and electro-optic materials for various photorefractive and holographic applications [2, 3]. Due to these attractive properties, considerable efforts have been devoted to the preparation and studies on the dielectric properties of BCT ceramics.

Various chemical routes have been used to obtain barium titanate ceramics, such as Pechini precursor route [4], hydrothermal [5–7], sol–crystal method [8], carbonate–oxalate (COBCT), gel–carbonate (GCBCT), and gel-to-crystallite conversion (GHBCT) [9], and low-temperature direct synthesis (LTDS) [10].

In this study, $Ba_{(1-x)}Ca_xTiO_3$ ($x = 0, 0.05, 0.10, 0.15$, and 0.20) powders were prepared by complex polymerization method (CPM) [11]. In the CPM problems such as high temperature and long reaction time, leading to inhomogeneous composition, are reduced because the synthesis occurs at low temperature and the immobilization of metal complexes in such rigid organic polymeric networks can reduce metal segregation, thus ensuring compositional homogeneity at molecular scale. This is of vital importance for the synthesis of multi-component oxides with complex compositions, since the chemical homogeneity, with respect to cation distribution throughout the entire gel system, often determines the compositional homogeneity of final multi-component oxides [11]. In previous paper, we evaluated the structural and optical properties of $Ba_{0.80}Ca_{0.20}TiO_3$ nanoparticles synthesized by CPM and annealed at different temperatures [2, 11, 12]. In order to evaluate the effect of different calcium content on the structural properties of the $BaTiO_3$ system presented in this study, samples were characterized using basic techniques such as X-ray diffraction (XRD) and Rietveld refinement, differential scanning calorimetry (DSC), and Raman spectroscopy.

V. D. Araújo (✉) · F. V. Motta · C. A. Paskocimas · M. R. D. Bomio
DEMAT, CT, UFRN, Av. Sen. Salgado Filho, 3000, Natal, RN CEP 59072-970, Brazil
e-mail: vicodantas@yahoo.com.br

A. P. A. Marques
UNIFESP, Rua Prof. Artur Riedel, 275, Diadema, SP CEP 09972-270, Brazil

E. Longo · J. A. Varela
LIEC, IQ, UNESP, Rua Francisco Degni s/n, Araraquara, SP CEP 14801-907, Brazil

Experimental

$Ba_{(1-x)}Ca_xTiO_3$ powders were prepared by CPM [11]. Briefly, titanium citrate was formed by dissolution of titanium(IV) isopropoxide into aqueous solutions of citric acid (CA). This solution was mixed in a stoichiometric molar proportion of 4:1 CA:titanium. Citrate solution was homogenized under constant stirring at temperature of ~80–90 °C, pH ~1.5. After complete dissolution $BaCO_3$ and $CaCO_3$ were added. Ammonium hydroxide was used to adjust the solution pH (pH 7–8). After solution homogenization, ethylene glycol was added to promote polymerization. The resulting polymer resin was then calcined at 300 °C for 4 h. The dark-brown powder obtained was then calcined at 1200 °C for 2 h to produce $Ba_{(1-x)}Ca_xTiO_3$ crystalline particles, where $x = 0$, 0.05, 0.10, 0.15, and 0.20. For simplicity, samples were named BT (pure $BaTiO_3$), BCT5, BCT10, BCT15, and BCT20.

The powders were characterized structurally in an X-ray diffractometer (Rigaku, Rotaflex RU200B) with Cu Kα radiation (50 kV, 100 mA, $\lambda = 1.5405$ Å), using a $\theta-2\theta$ configuration and a graphite monochromator. The scanning range was between 10° and 80° (2θ), with a step size of 0.02° and a step time of 5.0 s. Rietveld analysis was performed using the Rietveld refinement program GSAS [13]. A pseudo-Voigt profile function was used. The thermal analysis was performed by DSC technique using thermal analyzer (NETZSCH, model 204 CELL) in nitrogen atmosphere at heating rate of 10 °C min^{-1}. Al_2O_3 was used as reference material during thermal analysis. Raman spectroscopy data were obtained at room temperature using RFS/100/S Bruker FT-Raman equipment attached to Nd:YAG laser promoting excitation light of 1064 nm with spectral resolution of 4 cm^{-1} and range of 0–1100 cm^{-1}.

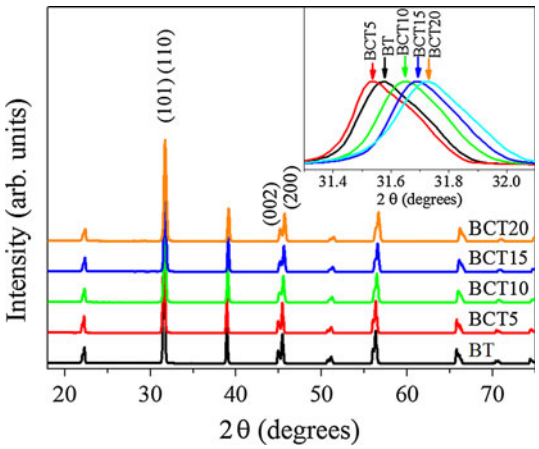

Fig. 1 X-ray diffraction patterns of $Ba_{(1-x)}Ca_xTiO_3$ samples. The *inset* shows the shift and broadening of (101) and (110) Bragg reflections

Results and discussion

Figure 1 shows the XRD patterns of $Ba_{(1-x)}Ca_xTiO_3$ samples. Tetragonal perovskite-type $BaTiO_3$ (ICSD no. 95436) was present in all samples. No secondary phase peaks were found. The inset in Fig. 1 shows a shift and broadening of (101) and (110) Bragg reflections with increasing Ca content, which can be attributed to differences of dodecahedra clusters formed by BaO_{12} and CaO_{12} network modifiers. These differences between clusters result in network deformation with loss of symmetry, generating disturbance in the crystalline network and, consequently, broadening of the peaks [14].

The cell parameter values for $Ba_{(1-x)}Ca_xTiO_3$ powders obtained from Rietveld refinement (Table 1), indicate a decrease in a and c cell parameters due to the substitution of Ba^{2+} (radii = 1.64 Å) by the smaller Ca^{2+} ion (radii = 1.34 Å) [15, 16]. Also, a nonlinear reduction of tetragonality (c/a) is observed with increase in calcium content. Samples presented small crystallite size ranging from 30.9 to 32.8 nm. Then, with the use of different characterization techniques, the effect of Ca on the structure of $Ba_{(1-x)}Ca_xTiO_3$ samples was investigated in order to clarify the reduction of tetragonality with increasing calcium content.

Figure 2 shows the DSC curves of $Ba_{(1-x)}Ca_xTiO_3$ samples. The BT sample presented an endothermic transition at 129.6 °C that corresponds to the tetragonal to cubic phase transition at the Currie point of $BaTiO_3$ [17]. With increasing calcium content, the Curie temperature

Table 1 Refinement parameters (S^2 and R_{Bragg}), lattice parameters a and c, tetragonality (c/a), crystallite size (D_{cryst}), Curie temperature (T_c), and heat of transition (ΔH) obtained from DSC curves of $Ba_{(1-x)}Ca_xTiO_3$ samples

Sample	S^2 (%)	R_{Bragg} (%)	a (Å)	c (Å)	c/a (Å)	D_{cryst} (nm)	T_c (°C)	ΔH (J g^{-1})
BT	2.27	8.90	3.9936(5)	4.0329(1)	1.0098(3)	32.8	129.6	0.539
BCT5	1.64	4.64	3.9889(1)	4.0283(9)	1.0099(1)	32.6	131.2	0.527
BCT10	1.90	5.01	3.9844(5)	4.0205(1)	1.0090(5)	30.9	133.4	0.064
BCT15	1.85	5.65	3.9785(2)	4.0170(3)	1.0096(8)	31.7	133.4	0.055
BCCT20	1.40	3.82	3.9694(4)	4.0065(1)	1.0093(4)	33.1	–	–

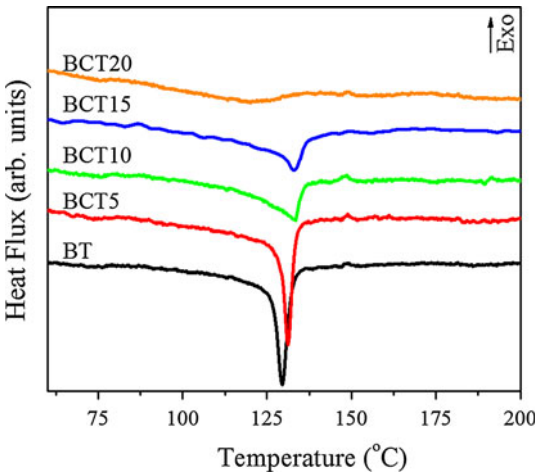

Fig. 2 DSC curves of $Ba_{(1-x)}Ca_xTiO_3$ samples

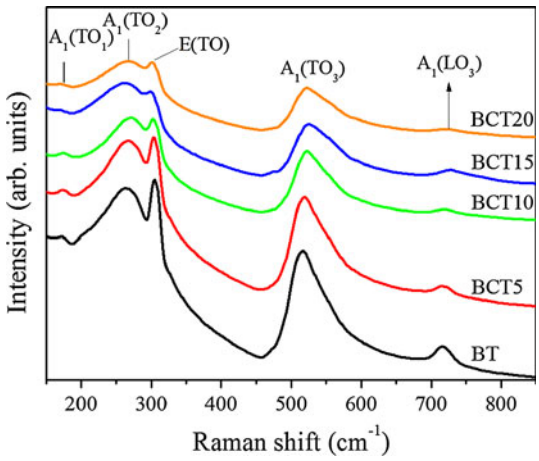

Fig. 4 Raman spectra using 1064 nm excitation line for $Ba_{(1-x)}Ca_xTiO_3$ samples

(T_c) shifts to higher values (Table 1) and the peak becomes less intense up to extinction for BCT20 sample. Völtzke and Abicht [18] showed the tetragonality of the $BaTiO_3$/$CaTiSiO_5$ system using the DSC technique. This study revealed that the addition of calcium into the BT matrix reduces tetragonality and, as a consequence, increases the Curie temperature. The heat of transition (ΔH) from tetragonal to cubic is shown in Table 1, revealing a decrease of ΔH with increasing Ca content, confirming that the addition of calcium into the BT matrix reduces tetragonality in accordance with XRD results presented above.

A more in-depth study on the tetragonality of $BaTiO_3$ samples can be achieved comparing thermal analysis and XRD techniques. Figure 3a presents Bragg reflections of (002) and (200) planes of BT sample. Theoretically 100 % tetragonal barium titanate has two separate peaks between theta 44° and 47°, and complete cubic barium titanate shows only one peak [19]. According to Baeten et al., tetragonality can be expressed comparing the relative peak height of the 002 and 200 peak, more precisely, the ratio of minimum between two peaks (B) and maximum (C) (as indicated in Fig. 3a). When compared with the heat of transition obtained from DSC curves, it could be inferred that tetragonality decreases with increasing Ca contents and that both techniques are in good accordance as seen in Fig. 3b.

Figure 4 shows the Raman spectra of samples, complementing the structural characterization. There are Raman active lattice vibration modes in tetragonal $BaTiO_3$ ($P4mm$), while there is no Raman active mode in cubic $BaTiO_3$ ($Pm3m$) [20]. Raman spectra showed the appearance of five distinct broad bands at 718, 520, 304, 267, and 175 cm^{-1}, which are characteristic of $BaTiO_3$ with tetragonal structure [21]. As the calcium content increases, the bands related to the vibrational modes of tetragonal $BaTiO_3$ become broader and less intense. This behavior is due to the fact that the addition of calcium into the $BaTiO_3$ matrix tends to promote a decrease in tetragonality. These

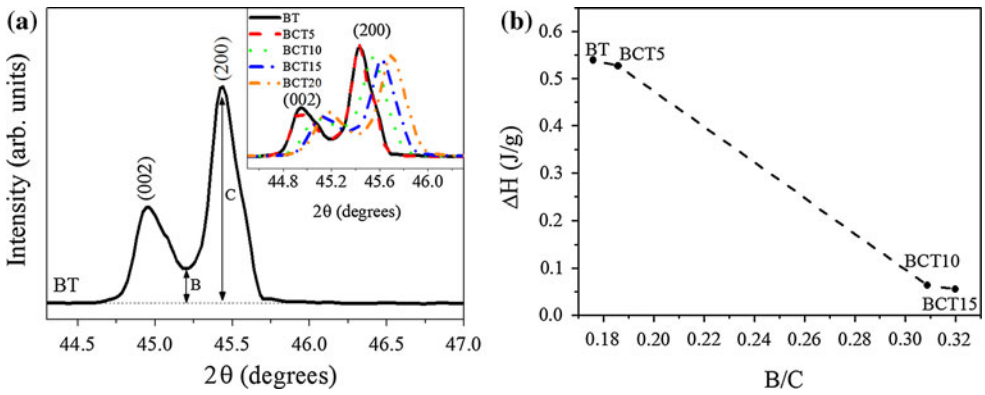

Fig. 3 **a** Bragg reflections of (002) and (200) planes of BT sample for the calculation of tetragonality (B/C). *Inset* variation of B/C and shift of (002) and (200) Bragg reflections with increasing Ca content. **b** Tetragonality relation expressed as B/C ratio compared to heat of transition from tetragonal to cubic for the samples

results are in agreement with XRD and DSC analysis, indicating that the substitution of Ba by Ca in the $BaTiO_3$ system results in a decrease in tetragonality.

Conclusion

The CPM proved to be efficient, simple, and advantageous in the synthesis of single-phase BCT compounds, due to low cost, low temperature, small reaction time, and allowing an atomistic distribution of cations throughout the matrix. XRD measurements revealed that differences between BaO_{12} and CaO_{12} clusters result in network deformation with loss of symmetry and that there is a decrease in lattice parameters and tetragonality with increasing calcium content. DSC results indicate that with increasing calcium contents, the Curie temperature (T_c) shifts to higher values and that the addition of calcium into the BT matrix reduces tetragonality. Finally, Raman spectra confirmed the XRD and DSC analyses, indicating that the substitution of Ba by Ca in the $BaTiO_3$ system results in a decrease in tetragonality.

Acknowledgements The authors would like to thank the financial support from the following Brazilian research financing institutions: Rede de Catalisadores Ambientais (RECAM), CNPq and FAPESP-CEPID 98/14324-8.

References

1. Ctibor P, Seiner H, Sedlacek J, Pala Z, Vanek P (2013) Phase stabilization in plasma sprayed $BaTiO_3$. Ceram Int 39(5): 5039–5048
2. Motta FV, Marques APA, Espinosa JWM, Pizani PS, Longo E, Varela JA (2010) Room temperature photoluminescence of BCT prepared by complex polymerization method. Curr Appl Phys 10(1):16–20
3. Kong X, Ishikawa Y, Shinagawa K, Feng Q (2011) Preparation of crystal-axis-oriented barium calcium titanate plate-like particles and its application to oriented ceramic. J Am Ceram Soc 94(11):3716–3721
4. Rai AK, Rao KN, Vinoth Kumar L, Mandal KD (2009) Synthesis and characterization of ultra fine barium calcium titanate, barium strontium titanate and $Ba_{1-2x}Ca_xSr_xTiO_3$ ($x = 0$; 0.05, 0.10). J Alloys Compd 475(1–2):316–320
5. Lee JH, Won CW, Kim TS, Kim HS (2000) Characteristics of $BaTiO_3$ powders synthesized by hydrothermal process. J Mater Sci 35(17):4271–4274. doi:10.1023/A:1004871915959
6. Ciftci E, Rahaman MN, Shumsky M (2001) Hydrothermal precipitation and characterization of nanocrystalline $BaTiO_3$ particles. J Mater Sci 36(20):4875–4882. doi:10.1023/A:1011828018247
7. Zhu W, Wang CC, Akbar SA, Asiaie R (1997) Fast-sintering of hydrothermally synthesized $BaTiO_3$ powders and their dielectric properties. J Mater Sci 32(16):4303–4307. doi:10.1023/A:1018663621241
8. Takeuchi T, Suyama Y, Sinclair D, Kageyama H (2001) Spark-plasma-sintering of fine $BaTiO_3$ powder prepared by a sol–crystal method. J Mater Sci 36(9):2329–2334. doi:10.1023/A:1017585209648
9. Jayanthi S, Kutty TRN (2004) Extended phase homogeneity and electrical properties of barium calcium titanate prepared by the wet chemical methods. Mater Sci Eng B 110(2):202–212
10. Zhang W, Shen Z, Chen J (2006) Preparation and characterization of nanosized barium calcium titanate crystallites by low temperature direct synthesis. J Mater Sci 41(17):5743–5745. doi:10.1007/s10853-006-0103-y
11. Motta FV, Marques APA, Escote MT, Melo DMA, Ferreira AG, Longo E, Leite ER, Varela JA (2008) Preparation and characterizations of $Ba_{0.8}Ca_{0.2}TiO_3$ by complex polymerization method (CPM). J Alloys Compd 465(1–2):452–457
12. Motta FV, de Figueiredo AT, Longo VM, Mastelaro VR, Freitas AZ, Gomes L, Vieira ND Jr, Longo E, Varela JA (2009) Disorder-dependent photoluminescence in $Ba_{0.8}Ca_{0.2}TiO_3$ at room temperature. J Lumin 129(7):686–690
13. Larson AC, Dreele RBV (1994) General structure analysis system (GSAS). Los Alamos National Laboratory Report LAUR 86-748. Los Alamos National Laboratory, Los Alamos
14. Souza AE, Silva RA, Santos GTA, Moreira ML, Volanti DP, Teixeira SR, Longo E (2010) Photoluminescence of barium–calcium titanates obtained by the microwave-assisted hydrothermal method (MAH). Chem Phys Lett 488(1–3):54–56
15. Chen J-C, Chen C-Y (2002) Growth of $Ba_{1-x}Ca_xTiO_3$ single-crystal fibers by a laser heated pedestal method. J Cryst Growth 236(4):640–646
16. Shannon R (1976) Revised effective ionic radii and systematic studies of interatomic distances in halides and chalcogenides. Acta Crystallogr Sect A 32(5):751–767
17. Badheka P, Qi L, Lee BI (2006) Phase transition in barium titanate nanocrystals by chemical treatment. J Eur Ceram Soc 26(8):1393–1400
18. Völtzke D, Abicht HP (1995) Investigations related to the incorporation of Ca^{2+} ions into the $BaTiO_3$ lattice. J Mater Sci 30(19):4896–4900. doi:10.1007/BF01154501
19. Baeten F, Derks B, Coppens W, van Kleef E (2006) Barium titanate characterization by differential scanning calorimetry. J Eur Ceram Soc 26(4–5):589–592
20. Suzuki K, Kijima K (2006) Phase transformation of $BaTiO_3$ nanoparticles synthesized by RF-plasma CVD. J Alloys Compd 419(1–2):234–242
21. Scalabrin A, Chaves AS, Shim DS, Porto SPS (1977) Temperature dependence of the A_1 and E optical phonons in $BaTiO_3$. Phys Status Solidi B 79(2):731–742